# Kinetics of random sequential adsorption of nearly spherically symmetric particles

Michał Cieśla[1,*] and Jakub Barbasz[1,2,†]

[1]*M. Smoluchowski Institute of Physics, Jagiellonian University, 30-059 Kraków, Reymonta 4, Poland*

[2]*Institute of Catalysis and Surface Chemistry, Polish Academy of Sciences, 30-239 Kraków, Niezapominajek 8, Poland*

(Received 15 November 2013; published 5 February 2014)

Kinetics of random sequential adsorption (RSA) of disks on flat, two-dimensional surfaces is governed by a power law with exponent $-1/2$. The study has shown that for RSA of nearly spherically symmetric particles this exponent is $-1/3$, whereas other characteristics typically measured in RSA simulations approach values known for disks with the increase of symmetry of the particles.

DOI: 10.1103/PhysRevE.89.022401 PACS number(s): 68.43.Fg, 05.45.Df

## I. INTRODUCTION

Random sequential adsorption (RSA) is one of the simplest and therefore one of the most commonly used numerical algorithms for modeling of irreversible adsorption processes [1–4]. It is also still actively studied and developed [5–7]. The algorithm is based on subsequent attempts to add a randomly placed particle to an adsorption layer. If the particle does not overlap with any previously added particles it is added to the layer. Otherwise, it is removed. One of the most important characteristics of an adsorption layer is its saturated coverage ratio—the ratio of surface covered by adsorbed particles to the whole collector area—when any further adsorption act is not possible. To be sure that a coverage is saturated, usually huge number of algorithm steps is needed, even when improved version of RSA is used [6]. To estimate saturated coverage ratio from relatively short simulation the kinetics of RSA layer growth has to be known. Since the very first studies by Feder [8] on spherical particles undergoing RSA procedure to form an adsorption layer on a two-dimensional flat collector, it has been observed that the coverage ratio kinetics is governed by the following power law:

$$\theta(t) = \theta_{\max} - At^{-\frac{1}{p}}, \tag{1}$$

where $\theta(t)$ denotes the ratio of space covered by adsorbed particles to the whole space of a collector after $t$ algorithm steps, $\theta_{\max} \equiv \theta(t \to \infty)$ is saturated coverage ratio, $A$ is some constant, and $p = 2$. For spherically symmetric particles, the above relation was analytically confirmed valid also by other investigators [9–11] and since then parameter $p$ is known to be equal to the dimension of a collector [12], which can also be a fractal [13,14]. The situation changes slightly for RSA of anisotropic particles, e.g., spheroids, spherocylinders, rectangles and similar [15–19], and even for fibrinogens [20]. In all these cases parameter $p$ in Eq. (1) has been found to be equal to 3 as long as particles are stiff [19,21]. In general, parameter $p$ is equal to the number of degrees of freedom of adsorbate particle [22]. The obvious question as to what is the limiting elongation between $p = 2$ and $p = 3$ scenario has been answered in Ref. [18]: for an ellipsoid having width to height ratio of $(1 + \epsilon)$ the border lies around $\epsilon \approx 0.25$. Interestingly, recent studies show that $p = 3$ also for tetramers [23] as well as for hexamers [24], and in the latter case $\epsilon$ is smaller than 0.25. As these shapes are often approximated by disks for numerical modeling purposes [5,25], it is possible that obtained results could lead to wrong conclusions [26,27]. Therefore, the aim of this study is to check which exponent $p$ describes RSA kinetics of nearly spherically symmetric molecules. To achieve this, a number of RSA simulation for particles of the growing number of symmetry axes was performed and analyzed.

## II. MODEL

Adsorbate particles are rings built of 5 to 40 identical disks of radius $r_0$. An example of rings is presented in Fig. 1. Such particles were thrown randomly on a flat square collector of a side size of $1000\,r_0$ according to RSA procedure [8,23,24]. Separate experiments were performed for particles of different sizes. During the simulation, temporary number of adsorbed particles $n(t)$ has been measured. For each type of molecules 100 independent simulations were performed and each of them included $10^5\,t_0$ steps, where $t_0 = 10^6/N\pi r_0^2$ is a dimensionless time unit equal to the ratio of collector surface to single particle surface. $N$ denotes the number of disks in a ring. Note that any specific value of the time unit does not affect exponent $p$ in Eq. (1) as long as it is proportional to the number of algorithm steps.

## III. RESULTS

Examples of monolayers built of different size rings are presented in Fig. 2. As the figure contains only a small fragment of the whole layer it is worth it to mention that the average number of adsorbed rings on the whole collector was 28 857, 14 691, and 6 020 for rings built of 5, 8, and 14 disks, respectively. The standard deviation did not exceed 10 particles.

### A. RSA kinetics

RSA kinetics measured for rings of different sizes are presented in Fig. 3. Validity of Eq. (1) has been confirmed for a wide range of simulation times. Exponent $p$, which corresponds to the slope of the lines in Fig. 3, almost does not depend on ring size and, within the studied range, is close to $p = 3$, even for the largest and most spherically symmetric particles. This is a highly unexpected result because with the

*michal.ciesla@uj.edu.pl

†ncbarbas@cyf-kr.edu.pl

 

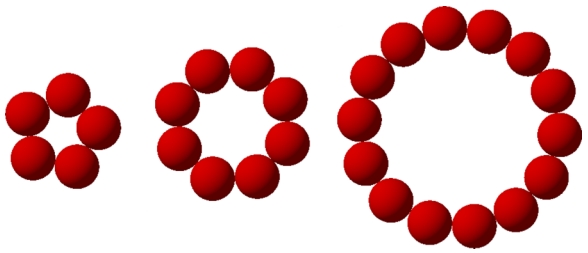

FIG. 1. (Color online) Example of rings built of 5, 8, and 14 identical disks.

particle shape approaching sphere, the exponent $p$ should approach the value of 2. However, it is generally possible that large rings do not approach disks in terms of properties measured using RSA simulations. To check if this is the case, other characteristics typically obtained from RSA simulations were measured and compared with the ones obtained from the RSA of disks.

### B. Saturated random coverage ratio

The surface covered by the ring is equal to $N\pi r_0^2$; however, the uncovered space inside the ring is also not available for subsequent particles adsorption. To compare obtained coverages with the disks adsorption case, the interior of the ring should also be counted as covered. Therefore, the total collector area occupied by a single ring built of $N$ disks is

$$S_N = Nr_0^2\left[\cot\left(\frac{\pi}{N}\right) + \pi\frac{N+2}{2N}\right]. \tag{2}$$

As mentioned at the beginning, the RSA simulation approaches saturated coverage after an infinite number of algorithm steps. Therefore, to find $\theta_{\max}$ the Eq. (1) is needed. Having determined the exponent $p$, let $y = t^{-1/p}$. Then Eq. (1) converts into $\theta(y) = \theta_{\max} - Ay$, where $A$ is a constant coefficient. Approximation of the linear relation for $y = 0$ gives the saturated random coverage $\theta_{\max} \equiv \theta(y = 0)$. Figure 4 presents saturated random coverage ratios for different ring sizes. Data for $N = 3$ and $N = 4$ were taken from Refs. [23] and [24], respectively. For trimers ($N = 3$), random saturated coverage ratio is only slightly lower than for disks. Significant drop of $\theta_{\max}$ for larger N is probably connected with the peculiar shape of medium-size rings, which effectively block slightly more space. For larger rings, saturated random coverage ratio, as expected, grows up to the value known for disks.

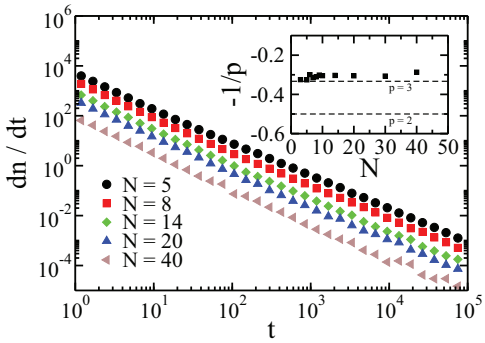


FIG. 3. (Color online) Increments of adsorbed particles versus number of RSA steps expressed in dimensionless time units $t_0$ for different sizes of rings. Inset shows the dependence of the exponent in Eq. (1) on ring size. Statistical error is smaller than the size of squares. Horizontal dashed lines correspond to $p = 2$ and $p = 3$.

### C. Available surface function

Available surface function can be defined as a probability of finding an uncovered space large enough to place there a subsequent particle. For small coverages, it can be approximated as

$$\mathrm{ASF}(\theta) = 1 - C_1\theta + C_2\theta^2 + o(\theta^2). \tag{3}$$

Expansion coefficient $C_1$ corresponds to the area blocked by a single particle, whereas $C_2$ corresponds to a cross-section of the surface blocked by two independent rings. Note that both of them are directly related to the second $B_2 = 1/2C_1$ and third $B_3 = 1/3C_1^2 - 2/3C_2$ viral coefficient of the equilibrium monolayer built of such particles [17,28]. Parameters $C_1$ and $C_2$ for rings were determined by fitting the Eq. (3) to the simulation data. Results presented in Fig. 5 show monotonic decrease of both the parameters down to the analytic values characterizing RSA of disks. In the case of $C_2$, the parameter drops even significantly below the expected value; however, it should be noted that expansion of ASF($\theta$) up to the second order is valid only for small $\theta$ and estimation of $C_2$ is much more sensitive to that range than of $C_1$. Here, for fitting purposes, we assumed that $\theta < 0.2\,\theta_{\max}$.

### D. Density autocorrelation function

Density autocorrelation function gives an insight into coverage structure and is defined as

$$G(r) = \frac{P(r)}{2\pi r\rho}, \tag{4}$$

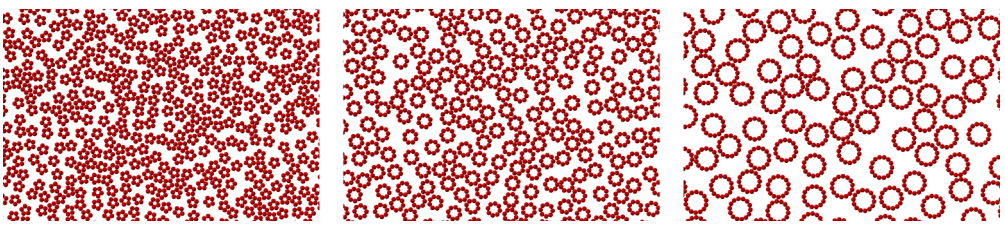

FIG. 2. (Color online) Examples of monolayers obtained using RSA procedure for rings built of 5, 8 and 14 identical disks.

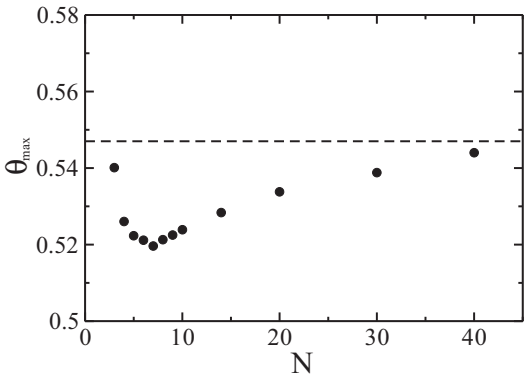


FIG. 4. Saturated random coverage ratio for rings of different sizes. Dashed line corresponds to saturated random coverage ratio for a monolayer built of disks [12,21]. Statistical errors are smaller than the size of dots.

where $P(r)dr$ is a probability of finding two particles in a distance between $r$ and $r+dr$. Here, the distance $r$ is measured between the geometric centers of molecules. As $\rho$ is the mean density of particles inside a covering layer, thus $G(r\to\infty)=1$. To compare density autocorrelations for different ring sizes, the length has to be rescaled and hence $r\to r/R_N$, where

$$R_N = r_0\left(\frac{1}{\sin\frac{\pi}{N}}+1\right) \tag{5}$$

is radius of the ring built of $N$ disks. The comparison of $G(r/R_N)$ is presented in Fig. 6. Again, values obtained for the largest rings approach the limit given by $G(r)$ for disks. This is yet another indication that random coverage properties for large rings match the ones for disks.

## IV. DISCUSSION

The difference between RSA kinetics for disks and for nearly spherically symmetric particles is counterintuitive, especially when considering results obtained by Viot *et al.*

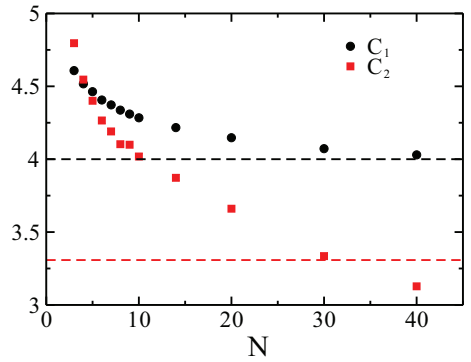


FIG. 5. (Color online) The ASF($\theta$) coefficients $C_1$ and $C_2$ for different ring sizes. Dashed lines correspond to their values for disks: $C_1=4$ and $C_2=\frac{6\sqrt{3}}{\pi}$. Statistical errors are smaller than the size of dots and squares.

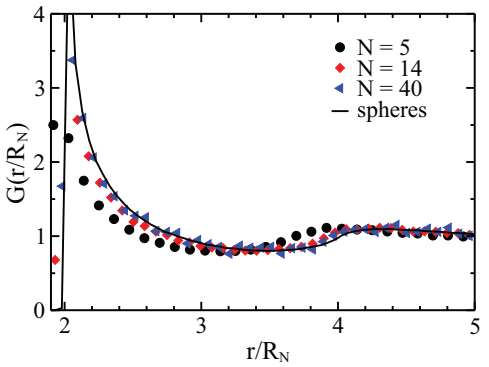


FIG. 6. (Color online) Density autocorrelation function for different ring sizes. The solid line corresponds to density autocorrelation function for disks.

[18] for convex particles. In that study, RSA kinetics for particles having the length-to-height ratio below 1.25 was closer to one for disks ($p=2$) than for elongated particles $p=3$. However, the behavior of RSA for concave particles can be significantly different [29,30]. Therefore, to find out where in this case the transition from $p=2$ to $p=3$ should occur in our case, we studied RSA for particles built of two identical, partially overlapped disks (see Fig. 7). As the ratio of particle width to height is $(1+\epsilon)$ the parameter $\epsilon$ can be used as an anisotropy measure. The RSA kinetics exponent defined in Eq. (1) for different $\epsilon$ is shown in Fig. 8. The transition from $p=3$ to $p=2$ for partially overlapped disks begins at $\epsilon\approx 0.02$, which is an order of magnitude lower than in the case of convex ellipsoids or spherocylinders [18]. It is worth noting that even for $\epsilon=0.1$, when particle looks almost spherical (see Fig. 7), the RSA kinetics still behaves as for elongated particles. In the case of previously simulated rings, the anisotropy reaches 0.02 for $N$ far larger than 100, which partially explains why the transition has not been observed in Fig. 3. On the other hand, the phenomenological explanation of the transition from $p=2$ to $p=3$ for elongated particles presented in Ref. [18] is still valid; however, the specific value of the border elongation between those two cases depends on the particular shape of a molecule and can be surprisingly low.

## V. SUMMARY

Although properties of saturated random coverages built of disks and nearly spherically symmetric particles are almost the same, the RSA kinetics is significantly different. Therefore, to obtain saturated random coverage ratio $\theta_{\max}$ on a flat

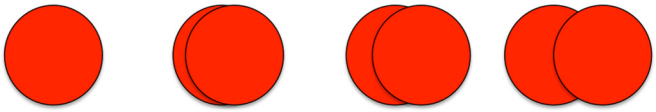

FIG. 7. (Color online) Examples of particles built of two, partially overlapped disks for anisotropy parameter $\epsilon$ equal to (from left) 0, 0.1, 0.25, and 0.5, respectively.

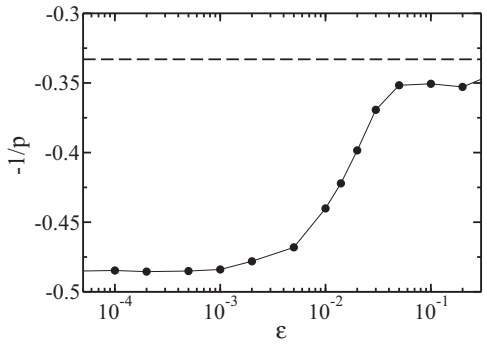


FIG. 8. The exponent from Eq. (1) dependence on anisotropy parameter $\epsilon$. Dashed line corresponds to $p = 3$. The statistical errors of presented data are below 0.003 and they are smaller than size of dots. The full line connecting dots has been drawn to guide the eye.

two-dimensional surface from a finite-time simulation, the $-1/3$ exponent in Eq. (1) should be used instead of $-1/2$, which characterizes RSA of disks. Although the difference between these two approximations is currently at the border of accuracy of typical experiments, development of new experimental techniques could make this difference significant. It was also shown that other characteristics typically measured in RSA simulation approach the value for disks along with the growth of particle symmetry level.

## ACKNOWLEDGMENT

This work was supported by Polish National Science Center Grant No. UMO-2012/07/B/ST4/00559.

[1] Z. Adamczyk, Curr. Opin. Colloid Interface Sci. **17**, 173 (2012).
[2] M. Rabe, D. Verdes, and S. Seeger, Adv. Colloid Interface Sci. **162**, 87 (2011).
[3] E. A. Vogler, Biomaterials **33**, 1201 (2012).
[4] B. J. Cowsill, P. D. Coffey, M. Yaseen, T. A. Waigh, N. J. Freeman, and J. R. Lu, Soft Matter **7**, 7223 (2011).
[5] C. Finch, T. Clarke, and J. J. Hickman, J. Comput. Phys. **244**, 212 (2013).
[6] G. Zhang and S. Torquato, Phys. Rev. E **88**, 053312 (2013).
[7] S. Živković, Z. M. Jakšić, I. Lončarević, Lj. Budinski-Petković, S. B. Vrhovac, and A. Belić, Phys. Rev. E **88**, 052131 (2013).
[8] J. Feder, J. Theor. Biol. **87**, 237 (1980).
[9] Y. Pomeau, J. Phys. A: Math. Gen. **13**, L193 (1980).
[10] R. H. Swendsen, Phys. Rev. A **24**, 504 (1981).
[11] V. Privman, J.-S. Wang, and P. Nielaba, Phys. Rev. B **43**, 3366 (1991).
[12] S. Torquato, O. U. Uche, and F. H. Stillinger, Phys. Rev. E **74**, 061308 (2006).
[13] M. Cieśla and J. Barbasz, J. Chem. Phys. **137**, 044706 (2012).
[14] M. Cieśla and J. Barbasz, J. Chem. Phys. **138**, 214704 (2013).
[15] J. Talbot, G. Tarjus, and P. Schaaf, Phys. Rev. A **40**, 4808 (1989).
[16] R. D. Vigil and R. M. Ziff, J. Chem. Phys. **91**, 2599 (1989).
[17] G. Tarjus and P. Viot, Phys. Rev. Lett. **67**, 1875 (1991).
[18] P. Viot, G. Tarjus, S. M. Ricci, and J. Talbot, J. Chem. Phys. **97**, 5212 (1992).
[19] S. M. Ricci, J. Talbot, G. Tarjus, and P. Viot, J. Chem. Phys. **97**, 5219 (1992).
[20] Z. Adamczyk, J. Barbasz, and M. Cieśla, Langmuir **26**, 11934 (2010).
[21] M. Cieśla, Phys. Rev. E **87**, 052401 (2013).
[22] P. Viot and G. Tarjus, Europhys. Lett. **13**, 295 (1990).
[23] M. Cieśla, J. Stat. Mech. (2013) P07011.
[24] M. Cieśla and J. Barbasz, J. Mol. Model. **19**, 5423 (2013).
[25] M. Aznar, A. Luque, and D. Reguera, Phys. Biol. **9**, 036003 (2012).
[26] M. Cieśla and J. Barbasz, J. Stat. Mech. (2012) P03015.
[27] J. J. Ramsden, G. I. Bachmanova, and A. I. Archakov, Phys. Rev. E **50**, 5072 (1994).
[28] Z. Adamczyk, *Particles at Interfaces: Interactions, Deposition, Structure* (Elsevier/Academic Press, Amsterdam, 2006).
[29] Y. Jiao, F. H. Stillinger, and S. Torquato, Phys. Rev. Lett. **100**, 245504 (2008).
[30] P. B. Shelke, S. B. Ogale, M. D. Khandkar, and A. V. Limaye, Phys. Rev. E **77**, 066111 (2008).